Original Article

SHM Structural Health Monitoring

Structural Health Monitoring
2024, Vol. 23(4) 2596–2608

DOI: 10.1177/14759217231208639
journals.sagepub.com/home/shm
Sage

Leak monitoring and positioning of pressurized water pipeline network

Yan Yupei[1*], Wang Shuoyuan[1*], Feng Hao[1], Gao Chao[2], Ma Jinyu[1], Li Jian[1] and Huang Xinjing[1]

Abstract

Due to the presence of numerous branches in the pressurized water pipeline network (PWPN), leak-caused negative pressure wave (NPW) has non-unique propagation path, so leak detection and positioning for PWPN is highly challenging. This paper proposes a leak monitoring and positioning method for PWPN based on the time delay matching of NPW propagation. Via introducing the NPW velocity equation, the PWPN is divided into short segments with equal NPW propagation duration, and then the shortest NPW propagation path from each discrete point, namely hypothetical leak point, to each deployed pressure transmitter, is efficiently numerically searched and then used to calculate the NPW arrival time and establish a contrastive time delay library (CTDL) in advance. A set of signal processing algorithm are developed to capture the NPW arrival time and compare these measured values with the pre-established CTDL to accurately position leak point in the PWPN. The effectiveness of this method is verified via leak localization experiments on a field PWPN with an area of 12 × 12 km and 1478 branches. The proposed method can achieve leak positioning with errors less than 100 m throughout the entire pipeline network when only six pressure transmitters are effective.

Keywords

Water pipeline network, leak detection, time delay matching, leak positioning

Introduction

Fluid pressure pipeline networks such as water supply and heating supply pipelines play an indispensable role in people's daily life. As urbanization develops, the scale of pipeline network construction is increasing, and corrosion is also becoming more and more serious. Pipeline leak incidents occur frequently, not only causing huge economic losses and resource waste, but also threatening people's life safety. For example, when a leak occurs in the urban water supply network, the total amount of water supply will increase, and the operating cost of the water supply network will also increase. At the same time, external pollutants are prone to enter the pipeline from the leak point, which will pollute the water and affect the normal water use of residents. For the heating supply pipeline network, the occurrence of sudden failure such as leak will lead to continuous heat loss. When the leak point is searched for a long time, the entire heating system may not be able to operate normally or even be paralyzed, which will cause great interference to the life of urban residents. Therefore, it is necessary to monitor the leak of pressurized water pipeline network (PWPN) in real-time, accurately alarm and locate the leak in the first time, so that remedial measures can be taken in a timely manner to minimize the losses.

At present, the most widely used method for leak monitoring of a single pressurized pipeline is the negative pressure wave (NPW) method.[1] When a leak occurs at a certain location in the pipeline, the fluid at the leak point is released due to the pressure difference between the inside and outside, causing a sudden mutation in the pressure value at that point and generating NPWs that can travel for tens of kilometers.[2] By arranging pressure sensors at both ends of the pipeline, the moment of pressure mutation can be detected, which is called the NPW arrival time. By calculating the time difference between signal mutations at both ends, the

[1]State Key Laboratory of Precision Measurement Technology and Instruments, Tianjin, China
[2]Tianjin Precision Measurement Technology Co., LTD, Tianjin, China

*These authors contributed equally to this work.

Corresponding author:
Huang Xinjing, State Key Laboratory of Precision Measurement Technology and Instruments, No 92 Weijin Road, Nankai District, Tianjin 300072, China.
Email: huangxinjing@tju.edu.cn

occurrence of a leak event and the location of the leak point can be determined. NPW-based leak detection and positioning method has developed to a very mature stage and has been widely applied. For the leak detection of a single pipeline, Cui et al.[3] proposed a pipeline leak detection method based on sequential testing; Kalman filter is used to preprocess the original pressure signal of the pipeline to improve the positioning accuracy, and the time difference method in NPW positioning is used to locate the leak point. In terms of signal processing, Jiang et al.[4] proposed a noise reduction algorithm based on variable modulus decomposition (VMD) and Hilbert transform, and used filtering technology and cross correlation coefficient to achieve NPW signal denoising. Han and Zhang[5] used the fast Independent Component Analysis algorithm to separate and decouple the denoised NPW signal into a source signal close to the original signal, and then perform leak localization. Due to the single propagation path of NPWs on a single pipeline, the deployment of pressure transmitters is convenient, and the NPW method has good leak detection and positioning effects.

However, on water and heating supply pipelines with a network structure, there is more than one propagation path for NPWs caused by leak. For small pipeline networks, pressure transmitters can be densely deployed to ensure that the pressure signals of each branch can be collected as much as possible. However, due to the non-unique propagation path of NPWs in the pipeline network, the traditional NPW leak detection method for a single long-distance pipeline is not applicable to the pipeline network. In order to overcome this difficulty, many scholars have conducted various explorations for small pipeline networks. Lin et al.[6] deployed pressure transmitters at various nodes of the small-scale experimental pipeline network, analyzed the arrival sequence of leak signals at each node, determined the leaking pipeline section, and located the leak point. Ozevin and Harding[7] used the principle of acoustic emission to measure the time difference between the leak sound signals received by sensors at different positions in the pipeline network, and combined with the theory of cross-correlation function to determine the location of the leak point in a small and simple pipeline network. Guo et al.[8] proposed a hydraulic transient detection method, which calculates the location of the leak point by exciting a transient water hammer wave at the end of a branch in a small pipeline network and measures the time of the breakpoint in the water hammer wave waveform.

The water and heating supply network is very large and has an enormous number of branches, resulting in a huge number of propagation paths for NPWs. It is extremely difficult to locate leaks solely based on time delay difference. The method used for leak detection and localization of small and simple pipeline networks has failed in large water transmission pipeline networks. Many scientists have tried artificial intelligence technology to conduct research on pipeline network leak detection and localization. Ma et al.[9] used the existing pressure, flow, and other information in the pipeline network as conditions for fuzzy decision-making to determine the leak status of the pipeline network. Jung and Lansey[10] proposed a pipeline leak detection method based on a Kalman filter, which samples and filters the flow value of the pipeline network throughout a day, and calculates the deviation between the measured and estimated flow values to achieve diagnosis of pipeline leak. Hu et al.[11] proposed a distributed detection method for pipeline anomalies based on element matrix triggering, which diagnoses the operating status of the pipeline network based on information such as valve opening and pipeline pressure. Sato and Mita[12] proposed a leak detection method using Support Vector Machine based on principal component analysis of the power spectrum of the leak signal, which can correctly identify the sound of pipeline leak. Jiao et al.[13] conducted time-frequency analysis on leak signals and proposed a BP neural network-based method for identifying pipeline leak acoustic signals. Priyanka and Thangavel[14] used digital twin technology to establish a leak feature extraction classifier based on ensemble local mean decomposition using pipeline network pressure data samples. Amini et al.[15] established an adaptive filter based on the principles of naive Bayesian classification and cumulative distribution function to identify leaks in oil and gas pipeline networks. Wachla et al.[16] divided the pipeline network into several regions and established a separate neural fuzzy classifier in each region to determine whether there was leak in the pipeline network in that region and adjacent areas. Costanzo et al.[17] divided the pipeline network into different regions based on the friction coefficient, and used Bayesian classification method to determine the leak zone based on the amplitude of changes in the friction coefficient of each region. It can be seen that the above methods can determine whether there is a leak in the pipeline network, but cannot achieve precise positioning of leaks; only a few of them can roughly determine the region of the leak point.

The structure of the pressurized water and heating supply pipeline network is very complex. Taking the urban heating pipeline network as an example, in order to meet the heating needs of multiple users, the pipeline must include a lot of branches. In densely populated areas, the pipeline branches will also increase accordingly. In this case, if the traditional NPW detection method is still to be used for pipeline leak detection, pressure transmitters need to be deployed at both ends of each branch, which is extremely expensive and not

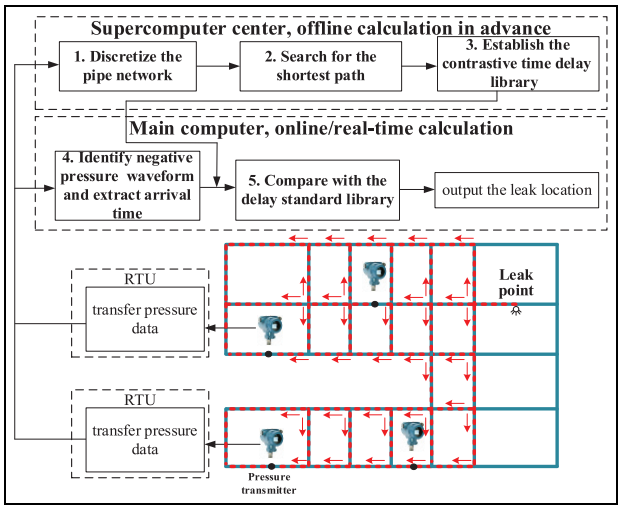

Figure 1. Block diagram of leak monitoring and positioning system for pipeline network with multiple negative pressure wave propagation paths.

feasible. However, when pressure transmitters are sparsely deployed, the multipath effect makes leak positioning extremely difficult.

Therefore, this paper proposes a leak detection and positioning method for water and heating supply pipeline networks based on shortest path planning and NPW propagation delay matching. First, the pipeline network is discretized with numerous nodes and shortest NPW path going through these nodes is searched. Then, based on the NPW velocity equation, the propagation duration of the NPW from each hypothetical leak point in the network to each pressure transmitter is calculated to build in advance a contrastive time delay library (CTDL). Pressure transmitters are sparsely deployed at several locations in the network to monitor the pressure in real time. Finally, when a real leak occurs in the pipeline network, the time delay array measured by each pressure transmitters is compared with the CTDL to determine the location of the leak point. This is an accurate rather than fuzzy method for positioning pipeline network leak points.

Leak positioning principle

As shown in Figure 1, the principle of this method mainly includes five parts: pipe network subdivision, shortest path search, establishment of CTDL, NPW identification and arrival time extraction, and time delay matching. First, the pipe network is subdivided into several discrete points according to the linear interpolation equation. Second, the Breadth-First Search (BFS) algorithm is used to calculate the shortest path along which NPWs propagate from each potential leak point to each pressure transmitter. Third, based on the NPW velocity equation, the NPW propagation duration on each shortest path is calculated to form a CTDL. The moment when the pressure waveform at the monitoring point begins to decrease is regarded as the NPW arrival moment. The arrival moment can be extracted from the recorded NPW waveforms. NPW propagation duration is defined as the value obtained by subtracting the leak occurrence absolute moment from this arrival moment. The leak occurrence absolute moment does exist but cannot be directly obtained. The above three steps can be executed in advance at the supercomputing center.

Fourth, NPWs are measured by each pressure transmitter and then sent to the pressure monitoring and data processing center; the algorithm of identifying NPWs and extracting the arrival time is executed in real time to monitor a real leak occurring at a certain point in the real pipeline network. Fifth, the delay array of the real NPW arrival time is compared with the CTDL from each hypothetical discrete leak point to the pressure transmitter location to determine the location of the leak point. These last two steps are carried out in real-time on the main computer of the pressure monitoring and data processing center.

The blue grid lines in Figure 1 represent the PWPN with pressure transmitters deployed at several known locations in the network. When a leak occurs at a certain location in the pipeline, NPWs propagate along different paths in the pipeline network. The red dotted line indicates the possible path of NPW propagation to the pressure transmitter. The pipe network is discretized in advance, and each discrete point is a potential hypothetical leak point. The supercomputing center calculates the shortest path from each discrete point (hypothetical leak point) to each pressure transmitter in advance, then obtains the shortest time of NPW propagation, and establishes the CTDL. When the system is working, the RTU (Remote Terminal Unit)[18] is used to connect to the pressure transmitter to monitor and collect pressure signals. The collected pressure signal is transmitted in real-time by the RTU to the main computer of the central station. The main computer detects the pressure waveform in real-time, identifies and extracts the arrival time of the NPW. Finally, the arrival time of NPWs measured by each pressure transmitter is compared with the CTDL to determine the location of the leak point.

Algorithm design

Pipe network discretization

The longitude and latitude coordinates of the two ends of a branch pipeline in the pipeline network are

(x_0, y_0), (x_1, y_1), and the inner diameter of the pipe branch between these two points is a constant value. Assuming the diameter of a certain section of pipeline is D and the pipe branch is divided into many discrete points with an interval of Δd_D. The coordinates of the discrete point q (x_q, y_q) can be expressed as:

$$\begin{cases} x_q = \dfrac{y_q - y_1}{y_0 - y_1} x_0 + \dfrac{y_q - y_0}{y_1 - y_0} x_1 \\ y_q = y_0 + q \dfrac{\Delta d_D}{\lambda \sqrt{1 + k_0^2}} \end{cases} \tag{1}$$

Wherein, $k_0 = \dfrac{x_1 - x_0}{y_1 - y_0}$ and $y_0 < y_1$; λ is the arc length along the longitude line on the Earth's surface when the latitude varies by one radian.

The propagation speed of NPW propagation is related to many parameters of the pipe, as shown in Equation (2). K is the elastic coefficient of the liquid, with the unit of Pa; ρ is the liquid density, with the unit of kg/m^3; δ is the wall thickness of the pipeline, with the unit of m; D is the inner diameter of each branch pipe section, with the unit of m; E is the elastic modulus of the pipe, with the unit of Pa; C_1 is the constraint coefficient of the pipeline. For water and heating supply steel pipelines, $K = 2.1 \times 10^9$ Pa, $\rho = 1.0 \times 10^3$ kg/m^3, $E = 2.0 \times 10^{11}$ Pa, $C_1 = 0.81$. δ and D of each pipe branch are provided by the water and heating supply pipeline company.

$$a = \sqrt{\frac{K/\rho}{1 + \frac{KD}{E\delta} C_1}} \tag{2}$$

The pipe diameter is denoted as D, and the minimum diameter in the pipe network is denoted as D_0. The pipe branch is divided into many subsections by many discrete points. For a pipe branch with a diameter of D, each subsection length is denoted as Δd_D; while for a pipe branch with a diameter of D_0, each subsection length is denoted as Δd_0. In order to be able to search the path corresponding to the shortest time delay via comparing the path point, it is necessary to modify Δd_D of the pipe branches with different pipe diameters according to the speed equation of NPW, so that the propagation duration of NPWs between any adjacent two points in the pipeline network is equal. Suppose that the NPW speed in a pipe with a diameter of D is a_D and the NPW speed in a pipe with a diameter of D_0 is a_0, then

$$\frac{\Delta d_D}{a_D} = \frac{\Delta d_0}{a_0} \tag{3}$$

According to Equation (2), there is

$$\Delta d_D = \Delta d_0 \cdot \sqrt{\frac{KC_1 D_{\min} + E\delta}{KC_1 D + E\delta}} \tag{4}$$

Finally, the pipeline network is discretized into n discrete points, whose numbers form the set $\mathbf{U} = \{i | i \in \mathbf{N}^*, i \leqslant n\}$. The pipeline network is equipped with p pressure transmitters, whose node numbers form a set $\mathbf{V} = \{v_j | j \in \mathbf{N}^*, j \leqslant p\}$, and $\mathbf{V} \subseteq \mathbf{U}$. The time delay standard library is $\mathbf{T} = \{t_{ij} | i, j \in \mathbf{N}^*, i \leqslant n, j \leqslant p\}$, t_{ij} is the time for the NPW to propagate from the discrete point i to the pressure transmitter at v_j when a leak occurs at the discrete point i.

Shortest path search

The BFS algorithm[19] is used to calculate the shortest path from each discrete point (potential leak point) in the pipe network to each pressure transmitter, and then the shortest time of NPW propagation can be obtained, and the CTDL is established. The specific process is divided into three parts.

Initialize discrete point information of pipe network. Adjacency matrix $C_{n \times n} = \{c_{\alpha\beta} | \alpha, \beta \in \mathbf{U}\}$ is established according to the connection relationship of the n discrete points obtained from discretization of pipe network, and,

$$c_{\alpha\beta} = \begin{cases} 1, & \text{point } \alpha \text{ and point } \beta \text{ are connected} \\ 0, & \text{point } \alpha \text{ and point } \beta \text{ are disconnected or } \alpha = \beta \end{cases} \tag{5}$$

Define a set of discrete point coordinates $P = \{(x_i, y_i) | i \in \mathbf{N}^*, i \leqslant n\}$, where (x_i, y_i) represents the longitude and latitude coordinates of the discrete point i. Define the set of discrete point access flags $\mathbf{F}$, $\mathbf{F} = \{f_i | i \in \mathbf{U}\}$, where $f_i = 0$ indicates that the discrete point i has not been accessed yet, and $f_i = 1$ indicates that the discrete point i has been accessed; all f_i are initialized to 0.

Select any discrete point $u \in \mathbf{U}$ in the pipe network as the potential leak point, and take the discrete point $v \in \mathbf{V}$, where a pressure transmitter is located as the end point of NPW propagation. Here $u, v \in \mathbf{N}^*$, $u \leqslant n$, $v \leqslant p$.

Search for the shortest path from u to v. The steps of the BFS algorithm are as follows:

Step 1: Define the cache array as H, initially containing only the element u.
Step 2: Sequentially access the discrete points in $\mathbf{U}$, and when accessing point m, sets its corresponding access flag variable f_m to 1.

Step 3: Judge the relationship between m and the first element of and H (denoted as $H[0]$) by checking the adjacency matrix **C**. If these two points are connected, add m to the end of H, and add $H[0]$ to array b_1, and also add m to array b_2.
Step 4: Determine whether the endpoint v is included in H. If not, remove the first element of H and execute **Step 2**. Otherwise, exit.

The pseudocode of the above algorithm is as follows:

```
H[0]←u; k←0; i←0
for each m∈U do
    f[m]←1
    if C[m, H[0]] = 1
        H[k]←m
        b1[i]←H[0]
        b2[i]←m
        k←k + 1;i←i + 1
  end
  if v∈H
    break
  end
end
```

After the traversal is completed, new arrays b_1 and b_2 are obtained, and the shortest path from u to v is obtained using a step-by-step backtracking method. The steps are as follows:

Step 5: Define the array *path* and the pointer variable array *point*. Initially, the *path* only contains the element v, and v is also assigned to the point.
Step 6: Record the position of the *point* in array b_2 as variable s.
Step 7: Add the element $b_1[s]$ to the array *path* and assign the value of this element to the array *point*.
Step 8: Determine whether the starting point u is included in the array *path* at this time. If not, execute **Step 6**. Otherwise, exit and output the shortest path – the array *path*.

The pseudocode of the algorithm is as follows:

```
b1[0,1,...,j], b2[0,1,...,j]
path[0]←v; point←v; p←0
for i←j to ←0 do
  if b2[i] = point
    s←i
  end
  p←p + 1
  path[p]←b1[s]
  point←b1[s]
  if u∈path
    break
  end
end
```

Calculate NPW propagation duration on the shortest path. After the shortest path from u to v is found, the sound velocity Equation (2) can be used to calculate the shortest NPW propagation duration t_{ij} for the NPW from discrete point $u = i$ where leak occurs to pressure monitoring point $v = v_j$, and t_{ij} is stored in the CTDL **T**. Then change the values of u, v and repeat the above procedures.

CTDL establishment

Due to the numerous branches of the pipeline network, there are multiple connecting paths between a leak point located at the discrete point i and the pressure transmitter j located at the node v_j. When real leak occurs, the NPW signal first received by the pressure transmitter is the one with the shortest propagation path, and the subsequent waveform will be superimposed and submerged in the tail wave. Assume that the shortest path includes a total of M branch pipe sections, each branch pipe section numbered as $k = 1, 2, 3,\ldots M$ has a length of $L^{(k)}$, a diameter of $D^{(k)}$, a pressure wave propagation velocity of $a^{(k)}$, and the propagation duration of NPW in each branch pipe section is $\tau_{ij}^{(k)}$, then

$$t_{ij} = \sum_{k=1}^{M} \tau_{ij}^{(k)} = \sum_{k=1}^{M} \frac{L^{(k)}}{a^{(k)}} \tag{6}$$

Among them, if the longitude and latitude coordinates of the two ends of the branch pipe section k are (x_A, y_A), (x_B, y_B), then the calculation equation for $L^{(k)}$ is:

$$L^{(k)} = R \cdot \arccos\left[\cos(y_A)\cos(y_B)\cdot\cos(x_A - x_B) + \sin(y_A)\sin(y_B)\right] \tag{7}$$

Wherein, R is the Earth radius.

The correctness of Equation (6) is verified using COMSOL finite element simulation software. The model is a portion of real pressurized heating supply pipeline network area of 4317 × 4142 m, as shown in Figure 2. The pentagram is the simulated leak point, and the dots are the location of 15 pressure monitoring points. The pipe network's branch length and location information are provided by the water and heating supply company and is imported into COMSOL to establish a simulation pipe network model. The internal medium is water, and the pipe wall material is set as structural steel.

The initial pressure of the pipeline network is set to 0.95 MPa, and at 1012 s, the pressure at the leak point drops by 0.02 MPa to simulate the NPW of a leak. The boundary conditions of the remaining pipeline endpoints are set to infinite extension. The pressure waveforms of the 15 monitoring points in the pipeline

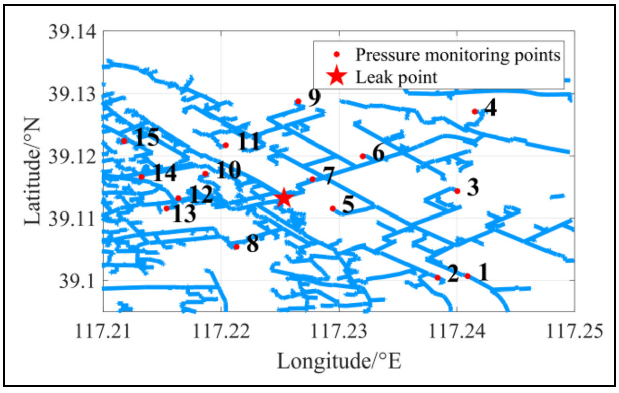

Figure 2. Pipeline network simulation model (horizontal scale: 1:57,560; vertical scale: 1:92,044).

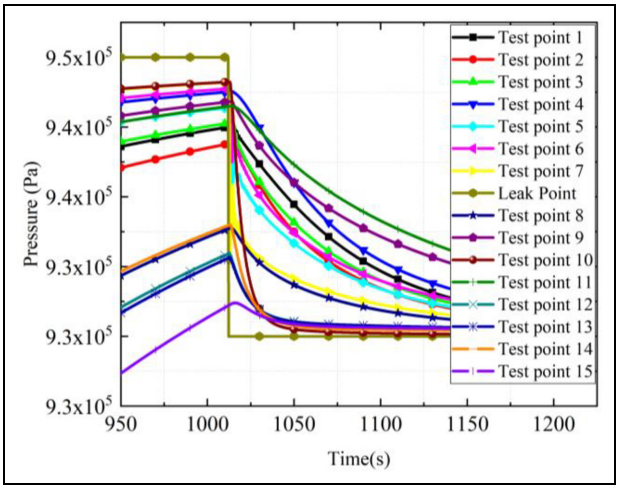

Figure 3. Simulation waveform.

network are shown in Figure 3. In the simulation, the entire pipeline network is pressurized from 0 Pa at the beginning until the pressure reaches a stationary value before the leak occurs. Therefore, the pressure waveform of each monitoring point in Figure 3 is showing an increasing tendency before the leak occurs. However, in reality, for an on-site pipeline network, this phenomenon does not exist.

By subtracting the leak occurrence time 1012 s from pressure drop moment, each NPW propagation duration from the leak point to the 15 monitoring points can be obtained. At the same time, the theoretical NPW propagation durations to 15 pressure monitoring points are calculated using Equation (6). Delay values obtained by two methods are listed in Table 1. It can be found that they are very close. Relative errors of 2/3 points are less than 10%. It can be concluded that when a pipeline network leaks, the NPW signal first received by the pressure transmitter propagates along the shortest path, which provides theoretical support for the algorithm design in this paper.

Table 1. Comparison of NPW propagation duration obtained by simulation and Equation (6).

Monitoring point	Distance (m)	Calculated propagation duration (s)	Simulated propagation duration (s)	Error (s)
1	3026.83	2.67	2.5	−0.17
2	3202.37	2.75	3	0.25
3	2740.71	2.31	2.1	−0.21
4	2898.57	2.53	2.7	0.17
5	1750.31	1.49	1.3	−0.19
6	1300.78	1.15	1	−0.15
7	553.13	0.49	0.3	−0.19
8	2204.04	1.83	2.1	0.27
9	2628.79	2.26	2.4	0.14
10	1272.00	1.06	1	−0.06
11	2980.41	2.56	2.8	0.24
12	1068.82	0.95	0.9	−0.05
13	1274.42	1.11	1.2	0.09
14	1529.95	1.31	1.3	−0.01
15	2242.79	1.92	1.6	−0.32

NPW: negative pressure wave.

Leak identification and NPW arrival time extraction

Leak identification. In field, there is noise in the pressure data collected by the pressure transmitter, so it is necessary to denoise the collected signal. Most widely used denoising methods include empirical mode decomposition (EMD) and wavelet decomposition.[20–22] The EMD method achieves denoising by removing the high-frequency components of the original signal, and then reconstructing the remaining modal components. However, removing the high-frequency components can easily cause distortion in the reconstructed signal.[23] The wavelet method denoise the original signal through wavelet transform decomposition and reconstruction, which can better characterize the non-stationary features of the signal (such as peaks and edges). Therefore, the wavelet denoising method is adopted for leak identification in this paper.

Figure 4 shows the effect of wavelet denoising on real pressure signals. The blue line represents the original pressure signal, and the red line represents the waveform after wavelet denoising. It is obtained by 8-layer wavelet transform of the original signal with a wavelet basis of 'db5'. It can be seen that wavelet transform can significantly reduce NPW signal noise without causing waveform distortion while preserving waveform time domain characteristics.

Through statistical analysis of the historical pressure data of the pipeline network, it is found that the

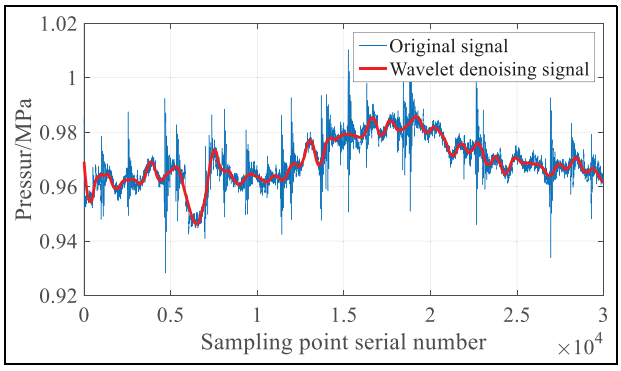

Figure 4. Wavelet denoising effect on real pressure signals.

variance of the leak signal is greater than 10^{-5} MPa, and the maximum peak-valley difference is greater than 0.013 MPa. Therefore, the thresholds of the two indicators are set to 10^{-5} and 0.013 MPa respectively. After denoising the signal, by calculating the variance, the NPWs with variances greater than 10^{-5} MPa are selected for the first time as the potential leak signals. Afterwards, the maximum peak valley difference is calculated of the initially screened waveform. If the maximum peak-valley difference of the measured NPW is greater than 0.013 MPa, it is considered that there is a leak.

NPW arrival time extraction. Haar wavelet can better reflect the mutation characteristics of the original signal. Figure 5 shows the original waveform containing NPW of the measured pipeline pressure and the corresponding composite signal using the first- and second-layer components of the Haar wavelet transform. It can be observed that the wavelet components of the large pressure drop section are more significant (as shown in the box highlighting area). Therefore, we consider to accurately locate the NPW arrival time of the identified NPW section by extracting the position of the modulus maximum of the first high-frequency component of the Haar wavelet transform.

Figure 6 is an example of using Haar wavelet to extract NPW arrival time. The blue line in the diagram represents the original pressure signal, and the red line represents the denoised signal after 8-layer wavelet transform. It is found that the modulus maximum point located by the first component of Haar wavelet is located at the point where the leak signal has the maximum descent slope, as shown by the purple point in the figure, and this moment is denoted as t_h. The peak time of the wavelet transform waveform is denoted as t_l, as shown by the green dot in the figure, Therefore, by averaging the corresponding times of these two points using α, β weighting coefficients selected based on the

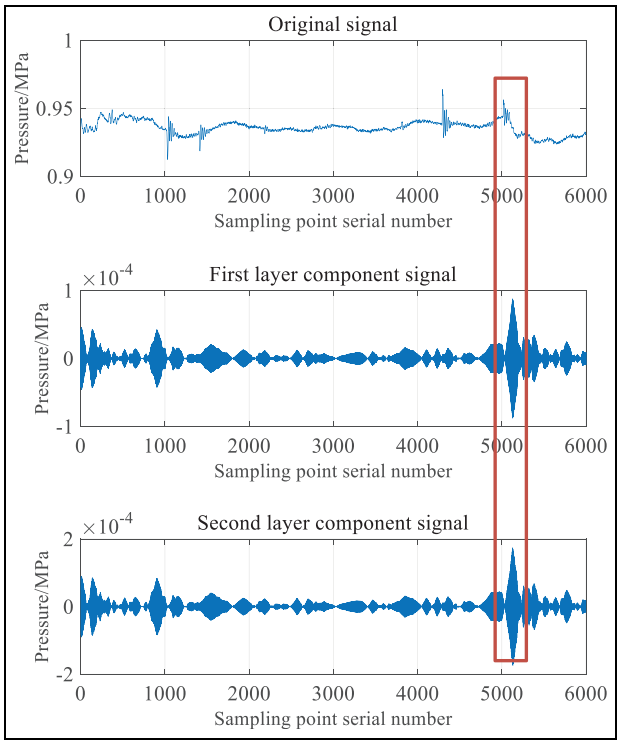

Figure 5. Haar wavelet decomposition and reconstruction of real negative pressure wave signal.

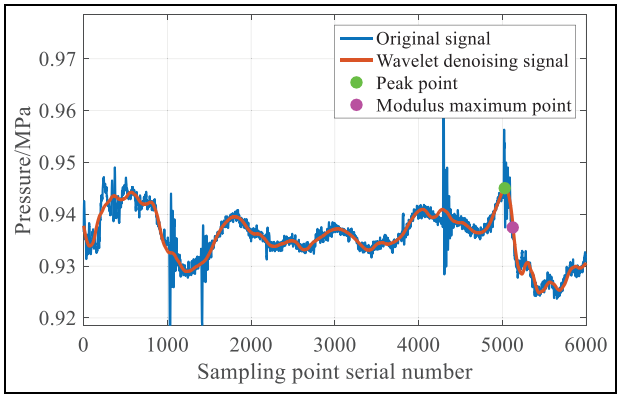

Figure 6. Diagram of extracting negative pressure wave arrival time via Haar wavelet transformation.

descending slope of the NPW, a more accurate NPW arrival time t_e can be obtained:

$$t_e = \alpha \cdot t_h + \beta \cdot t_l \tag{8}$$

The slope at the maximum value of the waveform modulus is defined as k_0, and this paper selects the value of α, β based on k_0. A larger $|k_0|$ means that the descent edge is steep and t_h is closer to the NPW arrival time, so α needs to be increased. Table 2 is the determination table of α, β. According to the historical

Table 2. Determination table of α, β.

Average value of k_0 (MPa/s)	α	β
$\geqslant -5.0 \times 10^{-4}$	0	1
-1.0×10^{-3} to -5.0×10^{-4}	0.25	0.75
-1.5×10^{-3} to -1.0×10^{-3}	0.5	0.5
-2.0×10^{-3} to -1.5×10^{-3}	0.75	0.25
$< -2.0 \times 10^{-3}$	1	0

data of pipeline leak, the k_0 measured is larger than -3.0×10^{-3} MPa/s. Therefore, the numerical interval in the first column of Table 2 is set to 5×10^{-4} MPa/s. After recording a leak waveform, k_0 of several sensor waveform modulus are calculated, and then the average value of these values is also calculated and used to determine the values of α, β according to Table 2.

Time delay matching

According to the method in the section 'Leak identification and NPW arrival time extraction', the NPW arrival time value corresponding to several pressure transmitters are extracted to form a time series τ_j ($1 \leqslant j \leqslant p$, p is the total number of pressure transmitters). The earliest time in the series is defined as $\tau_{\min}$, which is subtracted from τ_j to obtain a new sequence t_j:

$$t_j = \tau_j - \tau_{\min}, \quad 1 \leqslant j \leqslant p \tag{9}$$

Since the leak occurrence absolute moment is unknown, it is necessary to translate t for the sequence t_j as a whole to approach the real NPW propagation duration. Via subtracting t and t_j from t_{ij} of the CTDL, the matching error E_i is calculated as Equation (10). And the n_1 points with the smallest E_i will be selected as the positioning results.

$$E_i = \sum_{j=1}^{p} \left[t_{ij} - (t_j + t) \right]^2 \tag{10}$$

The following introduces how to select the optimal translation value t. Considering that the propagation time of NPW is within 20 s, the values of t is taken from -10 s to 10 s in sequence, with a step of 0.1 s. Whenever the value of t changes, a leak location is performed and the coordinates of n_1 positioning results are obtained. When the time translation value is t, assuming the positioning results are (x_1, y_1), (x_2, y_2), …, (x_{n1}, y_{n1}). The sum of Euclidean distances between any two coordinates, denoted as d_t, can be calculated as

$$d_t = \sum_{i=1, i \neq j}^{1 \leqslant i \leqslant n_1} \sqrt{(x_i - x_j)^2 + (y_i - y_j)^2} \tag{11}$$

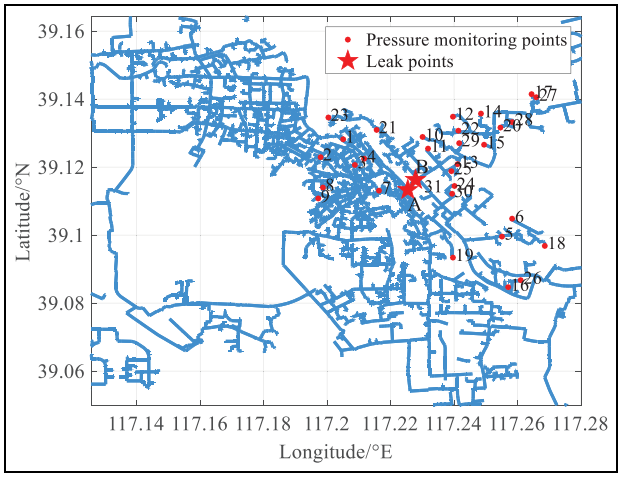

Figure 7. Experimental pipeline network's map (horizontal scale: 1:191,585; vertical scale: 1:244,154).

By sweeping t, several different d_t values are obtained. We use the t corresponding to the minimum d_t as the optimal translation time and n_1 positioning coordinates under this time translation time are output.

Experiment

Verification experiment of leak localization is carried out on a PWPN in the city of Tianjin. The pipeline network map is shown in Figure 7. The size of the pipeline network area is 12.453 × 12.696 km. The network includes 1478 pipeline branches and has a total length of 465341.3 m. The pipe diameter ranges from 33.7 to 1820 mm. A total of 31 pressure transmitters, numbered 1–31, have been deployed in the area. Among them, the straight-line distance between adjacent pressure transmitters varies from 300 to 5500 m. The interval with equal NPW propagation duration between discrete points in the entire pipeline network when calculating the CTDL is 10–20 m, and the network is subdivided by 45,999 discrete points. The on-site photos of the water leak test experiment of the PWPN are shown in Figure 8. Leak test at two locations is carried out. The coordinates of the leak testing points are point A (117.225°E, 39.113°N) and point B (117.228°E, 39.116°N), respectively. In this experiment, an outlet is welded to the pipeline network and a valve is installed. By opening the valve to drain water, the pipeline leakage is simulated, and the leakage rate is 5.89 L/s. The collected pressure signal is transmitted in real-time by the RTU to the main computer of the central station. In this experiment, the sampling rate of pipeline pressure is 20 Hz and there are a total of 72,000 sampling points per hour.

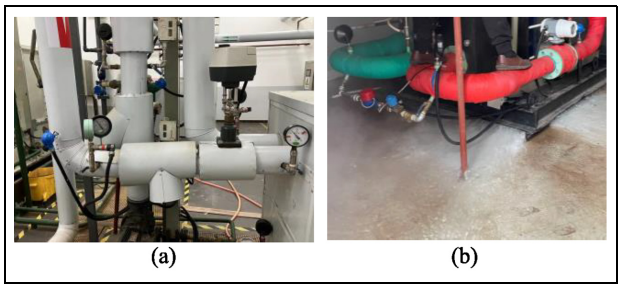

Figure 8. Experiment field of pipeline network leak positioning test. (a) Pipe photo in a station and (b) leak photo.

Results and discussions

Firstly, we analyze the leak pressure waveform and positioning results of leak point A testing. There are six pressure transmitters that successfully identified pipeline leak, namely pressure transmitters 1, 2, 4, 7, 29, and 31. The waveform of the leak section is shown in Figure 9. The other transmitters are unable to identify effective NPW signals due to being too far from the leak point. Haar wavelet transform is performed on the leak waveform to extract the modulus maximum of the first high-frequency component. The average value of k_0 is calculated as -1.1×10^{-3} MPa/s. According to Table 2, the weighting coefficient in Equation (8) is set as $\alpha = 0.5$, $\beta = 0.5$. The NPW arrival time of each waveform is calculated and shown as the red dots in Figure 9, which are 9:53:23.55, 9:53:23.65, 9:53:21.95, 9:53:20.35, 9:53:22.05, and 9:53:20.35, respectively.

From Figure 9, it can be seen that there is an error between the arrival time of the NPW extracted from the waveforms and the leak-caused pressure drop moments of Pressure Transmitter 1 and Pressure Transmitter 31. This is because the extraction of the NPW arrival time is done automatically by the computer, and the same algorithmic parameters are used for all the pressure transmitter's waveforms, namely α and β in Equation (8). Sometimes the error of the moment identified by such an automated program is greater than the error identified by a manual search method. However, the identification speed of the former is fast and real time, while the identification speed of the latter is very slow, so the latter is not competent for the real-time leak monitoring needs of the field.

The matching program is run to calculate the delay deviation E_i of each discrete point using Equation (10). For the leak testing at point A, 25 points with the smallest deviation E_i are selected as the positioning results for each time translation t, and the positioning results under different time translation values are shown in Figure 10. It can be seen that there are differences in positioning error with different translation values. The case where the error of the positioning points is the smallest is selected as the final positioning result, and the detailed map of the positioning points are shown in Figure 11; the time translation value t is -1.724 s. The 25 dots in the map are the discrete points with the smallest delay matching error, and the red pentagram is the actual leak point. It can be seen that the detected points are located near the leak point, and the positioning is successful, with an average positioning error of 41.2 m.

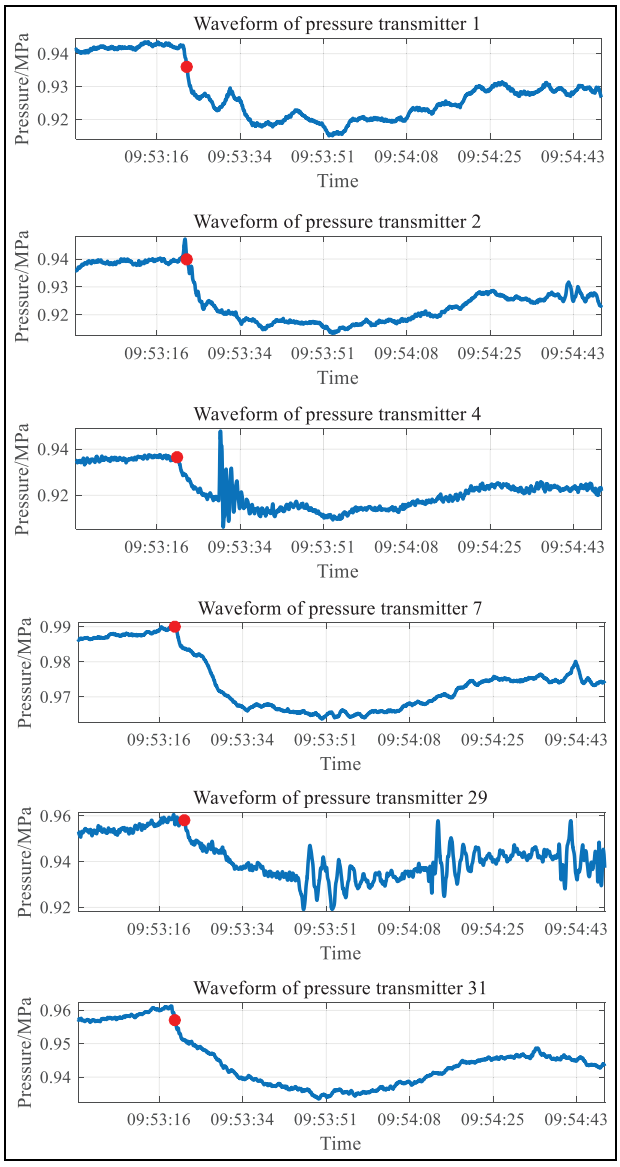

Figure 9. Pressure waveform caused by leak at point A; the red dot denotes the extracted leak moment.

For leak point B testing, the pressure transmitters 1, 2, 4, 7, 29, and 31 can correctly identified the leak, and the waveform of the leak-caused NPW is shown in Figure 12. The NPW arrival time extraction program and Equation (8) are used to calculate the leak occurrence time using each waveform. The average value of

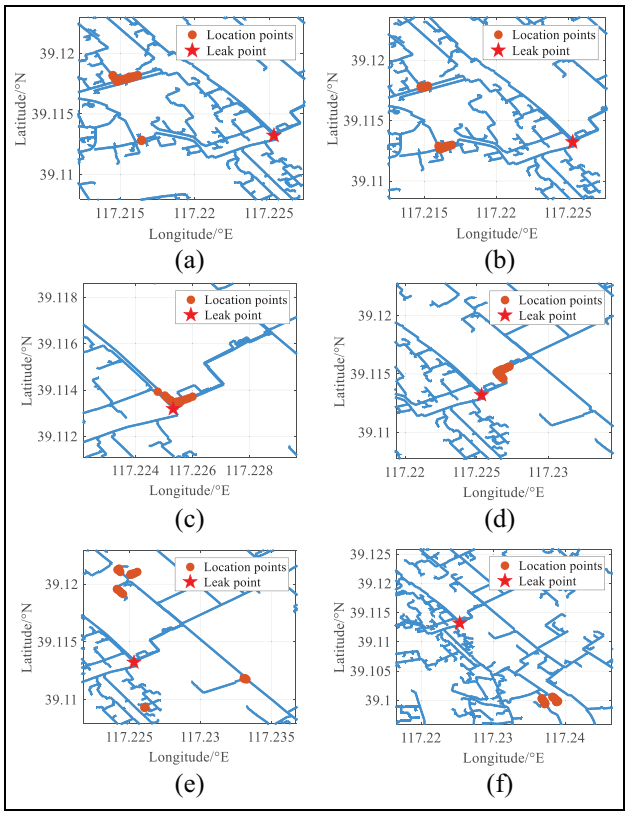

Figure 10. Positioning results with different time translation values (leak point A). (a) $t = -8.6207$ s, (b) $t = -5.8621$ s, (c) $t = -1.7241$ s, (d) $t = 0.3448$ s, (e) $t = 1.0345$ s, and (f) $t = 2.4138$ s.

k_0 is calculated as -4.2×10^{-4} MPa/s. According to Table 2, the weighting coefficient in Equation (8) is set as $\alpha = 0$, $\beta = 1$. The arrival times of the NPWs are calculated and shown as the red dots in Figure 12, which are 10:31:41.45, 10:31:43.57, 10:31:40.225, 10:31:41.35, 10:31:36.875, and 10:31:37.075, respectively.

The matching program is executed to calculate the delay deviation E_i of each discrete point according to Equation (10). Similarly, for the leak testing at point B, 25 points with the smallest deviation E_i are selected as the positioning results, and the positioning results under different time translation values are shown in Figure 13. The final localization results are shown in detail in Figure 14, where the time translation value t is -3.103 s. The 25 dots in the figure are the discrete points with the smallest delay matching error, and the red pentagram is the real leak point. It can be seen that the predicted points are located near the real leak point B; the positioning is successful with an average positioning error of 86.7 m.

Conclusion

Owing to the presence of multiple branches in the PWPN, leak detection and positioning based on NPW propagation in the pipeline network is highly challenging. This paper proposes a leak positioning method for PWPN based on the time delay matching of NPW propagation, and the feasibility of the proposed method is verified through actual pipeline network leak experiments. Main conclusions are as follows:

(1) Via introducing the NPW velocity equation, the water pipeline network is divided into short segments with equal NPW propagation duration, thereby transforming the shortest path search into the least number of discrete point search, and ensuring the accuracy and efficiency of establishing the CTDL.
(2) Finite element simulation is used to model the NPW propagation in a real large PWPN. The propagation duration of the leak-caused NPW from the leak point to each monitoring point on the

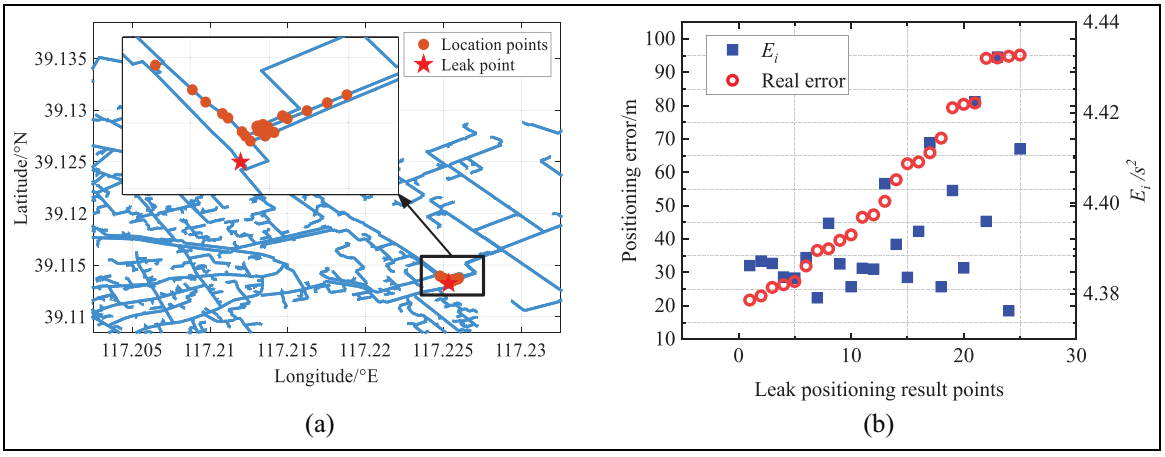

Figure 11. Leak positioning results of leak point A. (a) Leak positioning errors in map and (b) leak positioning error values.

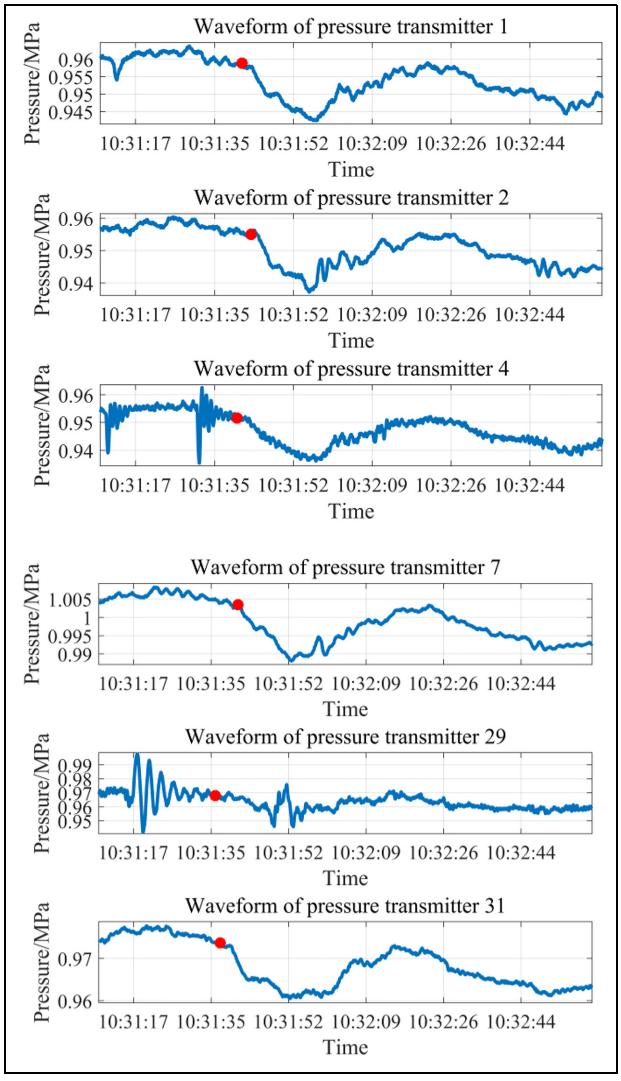

Figure 12. Pressure waveform caused by leak at point B; the red dot denotes the extracted leak moment.

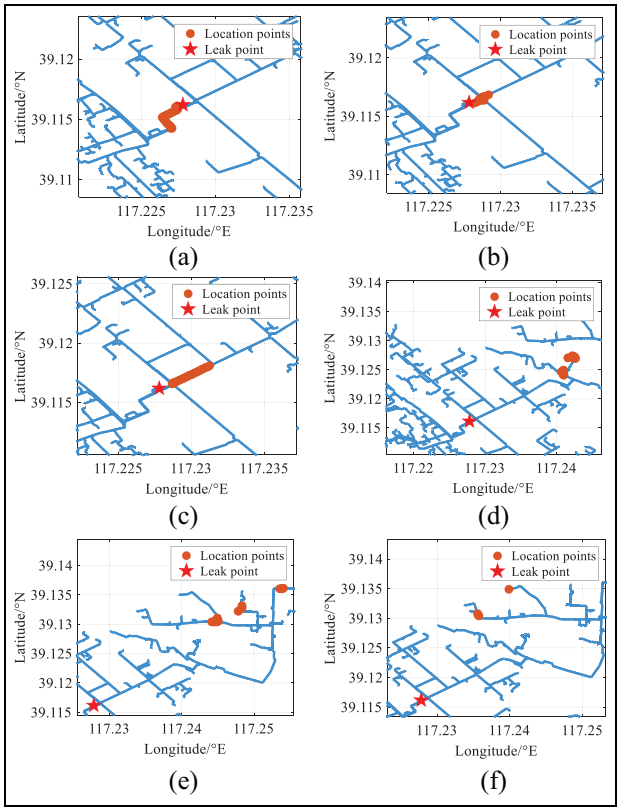

Figure 13. Positioning results with different time translation values (leak point B). (a) $t = -5.8612$ s, (b) $t = -3.1034$ s, (c) $t = -2.4138$ s, (d) $t = 0.34483$ s, (e) $t = 2.4138$ s, and (f) $t = 3.1034$ s.

pipeline network is calculated to verify the correctness and accuracy of the established CTDL.

(3) A complete set of detailed procedures of pipeline network leak localization have been designed, including pipe network discretization, shortest path search, CTDL establishment, leak identification, NPW arrival time extraction, and time delay matching. By monitoring pressure variations at only several points in the large pipeline network and implementing the designed signal processing algorithm, leak-caused NPW arrival time is captured and used to match the pre-established CTDL, and then leak localization can be achieved.

(4) Leak localization experiments have been conducted on a field pipeline network with an area of 12 × 12 km, 1478 branches, a total length of 465341.3 m, and six effective pressure monitoring transmitters. Localization of leaks for the entire pipeline network can be achieved with positioning errors of 41.2 and 86.7 m for two leak tests, indicating that the proposed method is correct and effective.

This method adopts an accurate non-fuzzy positioning principle and avoids installing numerous pressure transmitters on all branches of large PWPN.

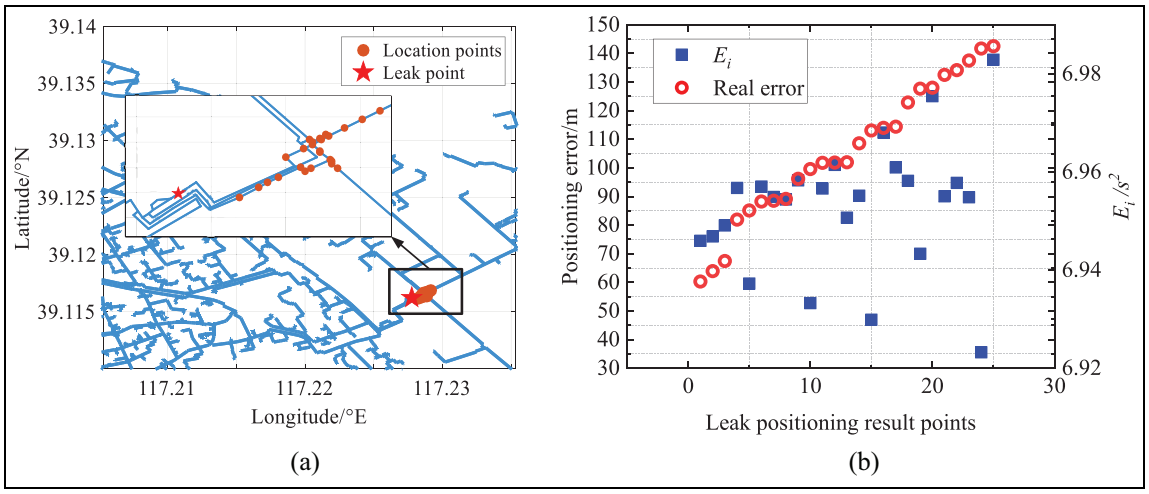

Figure 14. Positioning results of leak point B. (a) Leak positioning errors in map and (b) leak positioning error values.

Declaration of conflicting interests

The author(s) declared no potential conflicts of interest with respect to the research, authorship, and/or publication of this article.

Funding

The author(s) disclosed receipt of the following financial support for the research, authorship, and/or publication of this article: This work is supported by National Natural Science Foundation of China under Grant 62073233, Natural Science Foundation of Tianjin under Grant 21JCQNJC00690 and State key laboratory of precision measuring technology and instruments project under Grant pilab2104.

ORCID iD

Huang Xinjing https://orcid.org/0000-0002-8964-8502

References

1. Li J, Chen SL, Huang XJ, et al. Review of leakage monitoring and quasi real-time detection technologies for long gas & oil pipelines. *Chin J Sci Inst* 2016; 37(8): 1747–1760.
2. Liu EB, Li CJ and Peng SB. Leak detection for oil pipeline based on negative pressure wave theory. *J Harbin Inst Technol* 2009; 41(11): 285–287.
3. Cui Q, Jin SJ, Wang LK, et al. Detection method for pipeline leakage based on sequential probability ratio test. *Acta Petrolei Sin* 2005; 26(4): 123–126.
4. Jiang Z, Xie JY, Zhang J, et al. Denoising method of pipeline leak signal based on VMD and Hilbert transform. *J Sens* 2023: 16.
5. Han WX and Zhang LZ. Research on pipeline multipoint leakage location based on the time difference location method. *J Vibr Shock* 2022; 41(24): 210–217.
6. Lin WG, Wu Z and Wang F. Research on leak detection and location of the ship piping network based on virtual acoustic siginal. *Ship Sci Technol* 2018; 40(7): 152–157.
7. Ozevin D and Harding J. Novel leak localization in pressurized pipeline networks using acoustic emission and geometric connectivity. *Int J Press Vessel Pip* 2012; 92: 63–69.
8. Guo XL, Ma HM, Wang T, et al. Research and development of hydraulic transient detection experimental system for pipe network fault. *J Water Conservancy* 2019; 50(3): 305–314.
9. Ma DZ, Hu XG and Sun QY. Fuzzy decision-making method for oil and gas pipeline leakage monitoring based on big dimension data. *Acta Automatica Sinica* 2017; 43(8): 1370–1382.
10. Jung D and Lansey K. Burst detection in water distribution system using the extended Kalman filter. *Procedia Eng* 2014; 70: 902–906.
11. Hu XG, Ma DZ, Sun QY, et al. Pipeline anomaly distributed detection based on element-matrix trigger mechanism. *Control Theory Appl* 2017; 34(8): 1035–1045.
12. Sato T and Mita A. Leak detection using the pattern of sound signals in water supply systems. In: *Proc. SPIE 6529, Sensors and smart structures technologies for civil, mechanical, and aerospace systems, San Diego, California, 2007*, vol. 6529, p. 9.
13. Jiao JP, Li Y, Wu B, et al. Research on acoustic signal recognition method for pipeline leakage with BP neural network. *Chin J Sci Instrum* 2016; 37(11): 2588–2596.
14. Priyanka EB and Thangavel S. Multi-type feature extraction and classification of leakage in oil pipeline network using digital twin technology. *J Ambient Intell Hum Comput* 2022; 13(12): 5885–5901.
15. Amini I, Jin YD and Chen TW. Adaptive naive bayes classifier based filter using kernel density estimation for pipeline leak detection. *IEEE Trans Control Syst Technol* 2023; 31(1): 426–433.
16. Wachla D, Przystalka P and Moczulski W. A method of leakage location in water distribution networks using artificial neuro-fuzzy system. *IFAC PapersOnLine* 2015; 48(21): 1216–1223.
17. Costanzo F, Fiorini Morosini A, Veltri P, et al. Model calibration as a tool for leakage identification in WDS: a real case study. *Procedia Eng* 2014; 89: 672–678.

18. Zhang X, Gu YG, Zhang SQ, et al. Research on state estimation of linear grid based on intelligent monitoring system. *Electr Meas Instrum* 2021; 58(10): 112–117.
19. Xu Q, Han W, Chen J, et al. Optimization of breadth-first search algorithm based on many-core platform. *Comput Sci* 2019; 46(1): 314–319.
20. Mounir N, Ouadi H and Jrhilifa I. Short-term electric load forecasting using an EMD-BI-LSTM approach for smart grid energy management system. *Energy* 2023; 288: 113022.
21. Zhao X, Zhang J, Pu R, et al. The continuous wavelet projections algorithm: a practical spectral-feature-mining approach for crop detection. *Crop J* 2022; 10(5): 1264–1273.
22. Fan H, Tariq S and Zayed T. Acoustic leak detection approaches for water pipelines. *Autom Constr* 2022; 138: 104226.
23. Yang B, Yang Z, Tian Z, et al. Denoising analysis of GNSS coordinate time series by combining EMD-HD and wavelet decomposition. *Acta Geodaetica et Cartographica Sinica* 2022; 51(9): 1881–1889.